Dynamics of Helicopters with Dissimilar Blades in Forward Flight

James M. Wang* Inderjit Chopra†

Center for Rotorcraft Education and Research
Department of Aerospace Engineering
University of Maryland
College Park, Maryland 20742

Abstract

The rotor blades on any helicopter are usally never identical in real life, however, most helicopter aeroelastic stability analyses assume the blades are identical. There is a need to examine this realistic problem of how blade-to-blade dissimilarities modify helicopter aeromechanical stability and hub loads. The effects of blade-to-blade dissimilarities, such unbalance in blade mass, and dissimilarities in blade stiffness and aerodynamics are examined systematically. The results are discussed quantitatively and qualitatively. A study on blade dissimilarity is carried out using a finite element analysis that includes rotor aerodynamics, elastic blade deformations, and body pitch and roll motions. Results show that dissimilarity in blades' inplane stiffness improves the regressing lag stability, but with some increase in rotor side forces harmonics and 1/rev torque load. Dissimilarity in flap stiffness has little effect on aeromechanical stability and hub loads. Dissimilarities in blades' mass and lift do not affect aeromechanical stability, but severely increase hub loads.

Introduction

Recently, Wang and Chopra examined the air resonance behavior of dissimilar rotors in hover [1] and in ground resonance [2]. The results surprisingly showed that dissimilarity in lag stiffness reduces the common hingeless rotors' regressing lag instability. However, at the same time, it destabilizes other lag modes. This discovery was similarly observed by Pierre and Murphy in the study of jet engine compressor blades with mistuned blade assembly [3]. References [3, 4] showed that a slight dissimilarity in compressor blades' torsional frequency helps stabilize the least damped mode and at the same time destabilizes the most stable mode. The effect is to bring the real part (decay rate) of the eigenvalues of the least stable mode and most stable mode closer together. Reference [3] also pointed out that at the same time the frequencies of the least and most stable modes also become farther apart. It was pointed out in Ref. [1] that the "total damping" in the system between the isotropic and dissimilar rotor seems to be conserved at any given rotor speed.

In Ref.[5], Weller experimentally investigated the effects of when the elastomeric dampers on a 4-bladed bearingless rotor have different stiffness in hover. Weller's data show an increase in rotor damping when the blades have dissimilar damper stiffness.

In Ref.[6], Hammond examined the effects of when one lag damper is inoperative on an articulated rotor in hover. The effects of multiple dampers failure was examined by present authors in Ref.[2]. The results show that when one damper is inoperative, the stability of the collective lag mode is not affected at all. However, the stability of the progressing, regressing and differential lag modes are reduced uniformly at all rotor speeds. But they are still more stable than when no mechanical lag dampers are used.

McNulty [7] pointed out that when the structural stiffnesses are different among rotor blades will introduce additional frequency peaks in the frequency spectrum to complicate modal indentification in experiments. This additional frequency peak observation was also pointed out in the mistuned compressor blade study of Ref.[3].

Even though dissimilarity in blades may help reduce air resonance instability [1], and also helps reduce compressor blade flutter [3], but it may cause

*Graduate Research Assistant

†Professor

Paper presented at the 17th European Rotorcraft Forum, Berlin, Germany, Sept. 24-26, 1991.

large increase in blades' oscillatory amplitude, vibration level and hub loads. It is unclear whether the increased amplitude is localized to the mistuned blade only, or it affects the amplitude globally. This question can be answered by solving coupled blades/body equations via time integration.

For the dissimilar blades problem, there are two interesting areas worth examining. One is the particular solution, which yields the steady state rotor response. This gives information on how dissimilar blades affect hub loads and vibration level. The other area worth examining is the homogeneous solution, which gives insights as to how dissimilar blades affect aeromechanical stability. In this paper, both issues will be addressed. Specifically, the aeromechanical stability of hingeless rotors with dissimilar blades will be examined in forward flight. Due to greater control power, less parts count and lower maintenance, future helicopters will most likely be equipped with hingeless or bearingless rotors. Hingeless and bearingless rotors are usually designed as soft-inplane rotors to achieve manageable bending stresses on the blades. However, soft-inplane rotors are susceptible to aeromechanical instabilities. Thus, there is a need to determine precisely the aeromechanical stability when there are dissimilarities in soft-inplane rotors.

Analysis Formulation

The elastic blade analysis for examining articulated, hingeless, and bearingless rotors with and without blade dissimilarities was implemented on the Univerity of Maryland Advanced Rotorcraft Code (UMARC) [1, 9]. The analysis is based on a finite element method in space and time. The blade is assumed as a slender elastic beam undergoing flap bending, lead-lag bending, elastic twist, and axial extension. This Bernoulli-Euler beam is allowed small strains, and moderate deflections. Due to the moderate deflection assumption, the equations contain nonlinear structure, inertia and aerodynamic terms. Typically, these contain at least second order geometric terms. The finite element derivation is based on Hamilton's principle in the weak form. The blade is discretized into a number of beam elements. Each element has fifteen degrees of freedom. Between elements there is continuity of displacement and slope for flap and lead-lag deflections, and a continuity of displacement for axial displacement and geometric twist. The model assumes a cubic variation in flap bending, lag bending, and a quadratic variation for twist [8, 9]. Quasi-steady strip theory is used to obtain the aerodynamic loads. Noncirculatory forces based on thin airfoil theory are also included.

Blade Response and Vehicle Trim

In forward flight the blades' response and vehicle trim are solved as one coupled system using the modified Newton method. First, a flap only, rigid blade, coupled nonlinear vehicle trim is calculated to derive the initial trim and control settings for the coupled elastic blade/trim problem. These initial values (θ_{75}, θ_{1c}, θ_{1s}, θ_{tr}, α_s, ϕ_s) are used to calculate a 6x6 Jacobian matrix that will subsequently be used as slopes (derivatives of 3 fuselage forces and 3 moments with respect to the above six control and trim settings) to update new guesses for control and trim settings to help reach a convergence in both blade response and vehicle trim.

In each iteration, blade response is solved via finite element in time method. The response is assumed periodic with a period of one rotor revolution. Each revolution is discretized into a number of time elements (usually 6 to 8). At each time gaussian integration point, a set of spatial finite element equations is derived for the blade. To reduce computation time, the spatial finite element equations are transformed to a few equations (typically 3 to 6) in the normal mode domain using the coupled rotating natural modes of the blade. These spatial equations at all the time gaussian locations are then assembled into a first order global finite element in time equation. The periodicity of response is imposed by connecting the first and the last time element. This first order global equation is then solved.

When all blades are identical, only the response for one blade needs to be solved. When the blades are dissimilar, each blade response must be normalized by its own normal modes and solve individually. The blade loads for each blade are calculated and summed at the hub. The resulting hub loads at the hub are transformed to vehicle's fuselage center-of-gravity. A converged trim solution means the six vehicle equilibrium equations (3 forces and 3 moment equations about vehicle cg) must be simultaneously satisfied. Since blade response has a faster convergence rate than the vehicle trim, hence, a converged solution in vehicle trim also implies convergence in blades' response.

Stability Solution Technique

The coupled blade/body stability solution is solved by linearize the nonlinear blade equations used in response calculation. Body equations that are coupled to the blades are now added to form a set of coupled, second order, linearized, homegeneous, perturbation equations. The free vibration mode shapes about the averaged steady state blade response are used to nor-

malize the linearized finite element equations. This reduces the blade equations to n-modal equations and the stability solution will yield the familiar foundamental flap, lag and torsional modes.

The linearized perturbation equations in matrix form becomes:

$$\left[\begin{array}{c|c} \mathbf{M}_{bb} & \mathbf{M}_{bf} \\ \hline \mathbf{M}_{fb} & \mathbf{M}_{ff} \end{array}\right] \left\{\begin{array}{c} \ddot{\mathbf{q}} \\ \hline \ddot{\mathbf{x}}_f \end{array}\right\} + \left[\begin{array}{c|c} \mathbf{C}_{bb} & \mathbf{C}_{bf} \\ \hline \mathbf{C}_{fb} & \mathbf{C}_{ff} \end{array}\right] \left\{\begin{array}{c} \dot{\mathbf{q}} \\ \hline \dot{\mathbf{x}}_f \end{array}\right\}$$

$$+ \left[\begin{array}{c|c} \mathbf{K}_{bb} & \mathbf{K}_{bf} \\ \hline \mathbf{K}_{fb} & \mathbf{K}_{ff} \end{array}\right] \left\{\begin{array}{c} \mathbf{q} \\ \hline \mathbf{x}_f \end{array}\right\} = \mathbf{0} \qquad (1)$$

Where $\mathbf{q}$ is the vector of blade modal degrees of freedom for all the blades, and x_f is the vector of fuselage degrees of freedom. $\mathbf{M}_{bb}, \mathbf{C}_{bb}, \mathbf{K}_{bb}$ are the blade mass, damping and stiffness matrices. They represent four identical equations describing the blade motions in the rotating frame. $\mathbf{M}_{bf}, \mathbf{C}_{bf}, \mathbf{K}_{bf}$ are the coupled blade–fuselage mass, damping and stiffness matrices. $\mathbf{M}_{fb}, \mathbf{C}_{fb}, \mathbf{K}_{fb}$ are the coupled fuselage–blade mass, damping and stiffness matrices. $\mathbf{M}_{ff}, \mathbf{C}_{ff}, \mathbf{K}_{ff}$ are the fuselage mass, damping and stiffness matrices.

Even though the equations describing the four blades in the rotating frame are same, but the objective of this paper is to examine the effects when the blades are dissimilar, hence, the values for I_{b_m}, C_{ζ_m}, and ω_{ζ_m} ($m\ th$ blade inertia, external lag damping, and non-rotating lag frequency) maybe different for the blades.

In forward flight analysis the periodic coefficients arise from cyclically varying aerodynamic loads across the rotor disk. For dissimilar rotors, additional periodic coefficients arise from structural dissimilarities. Floquet analysis or time integration technique are used to solve the periodic system.

For dissmilar blade analysis, such as the effects of when one lag damper is inoperative, very surprisingly, the familiar constant coefficient approach used in fixed frame fails to yield descent results [2]. Constant coefficient approach can predict the stable modes quite accurately, but it fails to capture the unstable modes, rather, it predicted the unstable modes as stable. Even when using as many as 80 azimuth locations for averaging, it still fails to capture the instablities.

The disadvantages of using time integration are: time consuming, and the integrated time responses require post processing, such as Moving Block analysis, to determine the modal frequencies and dampings. But the advantage is the results are more physical and it can allow all the nonlinear terms to be kept. The disadvantage of Floquet analysis is the calculated modal frequencies are multi-valued and require additional efforts for determining the actual frequency Ref.[1]. But the advantage is it yields the decay rate directly which tells whether the modes are stable or unstable.

For the mistuned compressor blade problem [3], perturbation eigen analysis method can be used because there is no periodic coefficient in the equations. The aerodynamics involve axial flow similar to hover, and the problem assumes no inertia coupling between the blades or with the engine mount, thus, the equations are solved in the rotating frame. In Ref.[3], the only dissimilarity among blades (56 blades) is the torsion stiffness. The dissmilarity is modeled by adding a perturbation term in the stiffness matrix ($K = K_o + \delta K$).

When the coupled blade/hub equations are written in the above manner (Eq. 1), they can be solved directly in the rotating frame using Floquet theory. The eigenvalues of the Floquet transition matrix determines the stability of the "system". It is interesting to point out that solving the above matrix equations in the rotating frame yields identical Floquet eigenvalues as if they were transformed to the fixed frame and then solved using Floquet theory in the fixed frame. The reason is that the rotor and body behave as a coupled system, and the stability of the system is independent of the reference frame. Therefore, the decay rates of the modes are same, except the physical interpretation of the mode shapes is different. The modal frequencies for the collective and differential lag modes and body modes are same whether the problem is solved in the rotating or fixed frame. But the modal frequencies for the cyclic lag modes will differ between rotating and fixed frame by a factor of plus and minus Ω/Ω_o. By knowing whether a progressive or regressive mode is expected, the eigenvector provides a guide as to add or subtract the imaginary part of the Floquet eigenvalues to obtain the true frequency.

Floquet theory always gives the frequency as a number less than $\Omega/2\Omega_o$, then multiple of $\Omega/2\Omega_o$ must be added to obtain the true frequency [1]. Therefore, the rotating frame Floquet frequency will always appear same as the fixed frame Floquet frequency. If the interest is purely looking at the decay rate to determine the system stability, then computation time can be save by simply solving the system via Floquet in the rotating frame. Solving it in the rotating frame also reduces the numerical error accrued from the extra fixed frame transformation.

To solve the system equations (1) via Floquet, eigen analysis, or time integration, they must be transformed into first order form,

$$\dot{\mathbf{Y}} = \mathbf{A}(\psi)\ \mathbf{Y} \qquad (2)$$

For example, for a 4-bladed rotor if only blade lag mode and body pitch and roll modes are used, then the state vector $\mathbf{Y}$ for the rotating frame system is:

$$\mathbf{Y^T} = [\dot{\zeta}_1, \dot{\zeta}_2, \dot{\zeta}_3, \dot{\zeta}_4, \dot{\alpha}_s, \dot{\phi}_s, \zeta_1, \zeta_2, \zeta_3, \zeta_4, \alpha_s, \phi_s] \quad (3)$$

Where ζ_1 is the lag displacement for blade 1, and ζ_2 is for blade 2. α_s and ϕ_s are rigid body pitch and roll angles. If the system is transformed to the fixed frame, then the state vector $\mathbf{Y}$ becomes:

$$\mathbf{Y^T} = [\dot{\zeta}_o, \dot{\zeta}_{1c}, \dot{\zeta}_{1s}, \dot{\zeta}_d, \dot{\alpha}_s, \dot{\phi}_s, \zeta_o, \zeta_{1c}, \zeta_{1s}, \zeta_d, \alpha_s, \phi_s] \quad (4)$$

Where ζ_o, ζ_{1c}, ζ_{1s}, and ζ_d are the collective, cosine, sine, and differential lag components, respectively. If blade flap and torsion modes are used, the state vector will include $\dot{\beta}, \dot{\hat{\phi}}$ and $\beta, \hat{\phi}$.

Time Integration

The first order linearized perturbation equation in rotating frame (Eq. 2) can be integrated in time to yield time responses for the blade and body motions. Time traces provide more qualitative insights than eigen analysis because they reveal what each blade and body degree of freedom is doing, and how the oscillatory amplitude and phase differ among the blades as a function of time. On the other hand, Floquet and eigen analyses examine the coupled coupled rotor/body system as a whole, and does not reveal what individual blade is doing, nor indicate which blade is going unstable. Furthermore, Floquet assumes the problem is periodic and average the stability over one revolution. Time integration provides helpful understanding, especially when there are blade dissimilarities. In this paper, the responses are integrate for 40 rotor revolutions. Uniform blade chordwise initial displacements are given for all blades. The numerical integration step size ($\Delta\psi$) must be selected smaller than π/ω, where ω is the highest frequency in the problem, to prevent alias problem in the time response.

Baseline Rotor Configuration

A hypothetical soft-inplane hingeless rotor is chosen for the parametric study. It is a four bladed rotor with blade structure and fuselage properties similar to the BO-105. The properties used for the analysis are given in Tables 1 and 2. The blades are treated as cantilever beams with blade root starting at 2% radius location. The UMARC code accepts blades with an arbitrary distribution of element properties along the blade; however, for this paper only blades with uniform spanwise properties are used. Five elements are used for each blade. Structural damping and lead-lag dampers are not included in the baseline configuration. The fuselage is modeled as a rigid body with pitch and roll degrees of freedom (α_s, ϕ_s). For the stability solution, three coupled rotating normal modes are used (first flap, first lag, and first torsion). The nominal operating speed for this rotor is chosen to be 424 rpm. At this rotor speed, the rotating fundamental natural frequencies of the blades are: flap frequency = 1.15/rev, lag frequency = .74/rev, and torsion frequency = 4.67/rev, which represent a typical soft-inplane hingeless rotor. The total number of eigen states from the Floquet analysis is 28. (It is a 4 bladed rotor system, and each rotor mode yields 8 states. Since three normal modes are used, this gives 24 states. Two rigid body modes are used, and each mode yields 2 states.) For this study, $C_T/\sigma = .07$ is used throughout, representing a typical thrust loading.

Results and Discussion

In this paper, a parametric study of six different rotors is conducted. Figures 1 through 7 present the lag mode stability results. The fixed frame lag mode dampings are plotted for advance ratio from $\mu = 0$ to $\mu = 0.3$. All stability results are presented in terms of a decrement ratio:

$$DECREMENT\ RATIO = -\frac{\sigma}{\Omega_{ref}} \quad (5)$$

The decrement ratio is defined as the real part of the complex eigenvalue with a negative sign, and nondimensionalized by the reference rotor speed. A positive value of decrement ratio represents a stable condition, where as a negative value represents instability.

Figures 9 through 14 give the harmonics of the fixed frame hub loads for the six rotors at $\mu = 0.2$. The axis system for the three hub forces and three moments are defined in Figure 8. The forces are normalized by steady rotor thrust. The moments are normalized by steady rotor torque. The 0th harmonic for F_Z and M_Z are not shown because they would equal 100%. Finally, Figures 15 and 16 present the time responses for two dissimilar rotors in hover. The traces are generated by integrating the linearized coupled blades/body perturbation equations (Eq. 1) for 40 revolutions.

Before delving into the stability results, a brief explanation of fixed frame lag modes is offered here. Collective, differential, progressing and regressing lag

modes are rotor natural modes in the inplane direction as seen by an observer standing on the ground in the nonrotating frame of reference.

Progressing lag mode is due to a coupling between the ζ_{1c} and ζ_{1s} motions. It appears as a forward whirling of the rotor mass in the same direction as the rotor's rotation. This is called a "progressive" forward whirling of the rotor center-of-mass. Using a 4-bladed rotor as example, this phenomenon is due to one pair of blades causes a lateral shift in rotor's center-of-mass due to ζ_{1c} motion, then the pair of blades located 90 degrees ahead causes a longitudinal shift in rotor's center-of-mass shift due to ζ_{1s}. Due to a time delay between the ζ_{1c} and ζ_{1s} motions, this sequential relay action appears to an outside observer as if the center-of-mass of the entire rotor is whirling forward in the direction of the blade rotation. The rate that the mass is whirling is the progressing mode natural frequency. The progressive whirling is illustrated in Ref.[2].

Regressing lag mode is also due to a coupling of the ζ_{1c} and ζ_{1s} motions. For an articulated or a soft-inplane hingeless rotor (ω_ζ/Ω less than 1/rev), the regressing lag also shows "progressive" forward whirling of the center-of-mass, but the whirling rate is at the regressing lag mode frequency. For a stiff-inplane hingeless rotor (ω_ζ/Ω greater than 1/rev), the regressing lag mode shows a regressive whirling of the rotor center-of-mass opposite to the direction that the rotor is spinning.

Figure 1 gives the stability results for the baseline hingeless rotor. It shows that the regressing lag mode is the least stable rotor mode. Progressing, collective, and differential lag modes are slightly more stable. Since structural damping is not included, therefore, all dampings originate from aerodynamics. The dampings reach a minimum at $\mu = 0.15$, and grow steadily as advance ratio is increased. The point of minimal lag damping corresponds to translational lift condition where minimal power is required to produce constant thrust. It is well known that lag damping is proportional to collective pitch. To sustain $C_T/\sigma = 0.7$, 8.5° collective pitch is needed at hover; while only 6.5° is needed at $\mu = 0.15$, and almost 9° is needed at $\mu = 0.3$.

In Figs. 9 through 14, the hub loads for baseline rotor have only 0th and 4th harmonics. 0th harmonics represent the steady forces and moments required to keep the helicopter in trimmed flight. The 4/rev harmonics are the vibratory loads due to it is a 4-bladed rotor in forward flight: each blade encounters the same aerodynamic asymmetry in one revolution, hence 4/rev loads.

Reduced Blade Lag Stiffness

The first dissimilar rotor case represents a rotor where lag stiffness (EI_Z) is reduced by 10 percent along the entire span for just one of the blades. The other three blades have the same lag stiffness as the baseline configuration. For all the dissimilar rotors used in this paper, blade number 2 was arbitrarily selected as the dissimilar blade. By reducing the inplane stiffness (EI_Z) of one blade, the regressing lag mode becomes more "stable," in particular at advance ratio less than 0.1. As shown in Fig. 2, the collective lag mode has become less stable. It seems that the energy feeding in from the coupled blades/body motion to destabilize the regressing lag mode has been channeled partially to other lag mode. As shown in the eigenvectors of Ref.[1], for dissimilar rotors, regressing, progressing, collective, and differential modes become highly coupled. For example, the collective mode shows almost equal participation from collective lag ζ_0 and reactionless lag ζ_d components. Similar is true for differential lag mode. Hence, for dissimilar rotors, the names collective and differential are more for tagging purpose, rather than describing the modal motions.

Figures 15a through 15c present the time responses for the reduced inplane stiffness rotor in hover. At t=0, all four blades are given identical chordwise displacements. Figure 15a shows the initial lag displacement is 2° for each blade. The initial flap and torsion responses at t=0 are non-zero because the collective pitch is at 8.5°, hence a chordwise displacement also introduces flap and pitch displacements. The time responses are shown for hover to illustrate that the out of phase oscillations are due to blade dissimilarities, and not due to forward flight. Because in hover, if all the blades are identical, the four blade responses will be identical.

In the first few rotor revolutions, all four blades have similar lag, flap, and torsion traces. But after three or four revolutions, the dissimilar blade (blade 2 which has softer inplane stiffness) starts to deviate away from the pack. As shown in Fig. 15a, blade 2 has longer oscillatory period because it is softer. The consequence is to ruin the rotor symmetry and causes an inplane excitation to whirl the rotor shaft. Figure 15a shows after five revolutions, the rotor induced noticeable body pitch and roll oscillations. The body motions grow steadily for about 10 revolutions, and they reach their peak around 20th revolution. Then, body motions start to decay because blade motions are decaying, too.

It is interesting to point out that the softer blade (blade 2) undergoes larger lead-lag amplitude as expected because it is easier to bend. Surprisingly, it is

the adjacent blade (blade number 3) that shows the second largest oscillatory amplitude, and not the opposing blade (blade 4). Instead, for the first 30 revolutions, blade 4 shows the smallest oscillatory amplitude, but after 30 revolutions, blade 1's motion becomes the smallest.

As time goes on, the phasings between all four blades become completely off. The consequence is to smear the familiar progressing, regressing, collective, and differential modes together. Now all the modes contain large ζ_o, ζ_{1c}, ζ_{1s}, and ζ_d components. This helps make all the modes loose their original identity and look more like each other. This effect can best be seen in the eigenvector diagrams of Ref.[1]. Due to this closer resemblence among the modes, their damping values also become closer together. As shown in Fig. 2, the least stable mode becomes more stable, and the most stable mode becomes less stable. If the dissimilarities are severe and random enough, the eigen structure of the modes may be destroyed and all four fixed frame lag modes may have almost same decay rate.

Increased Blade Lag Stiffness

Figure 3 shows the effects of increasing the inplane stiffness of one blade by 10%. Near hover condition, regressing lag is improved even more than the reduced inplane stiffness rotor (Fig. 2). But for advance ratio greater than 0.1, the improvements for the two cases are comparable.

The consequence of having one blade softer or stiffer in the lag direction may be utilized as an advantage from the air resonance stability point of view, because it allows a sharing of the body excitation energy between regressing and other lag modes. However, these dissimilar rotors will affect hub loads and vibrations. Hub load results in Figs. 9 through 14 show appearence of 2/rev harmonics in rotor drag force and side force. Since the amplitudes are less than 1%, hence, they are relatively weak. However, large 1/rev harmonic appears in rotor torque, M_Z. This is due to the dissimilarity in inplane stiffness introduces out of phase lead-lag motion among all the blades. This causes oscillatory torque load on the main shaft.

The inplane drag and side forces created are 2nd harmonics in nature because it is a 4-bladed rotor. When two opposing blades swing toward the same side of the rotor disk, rotor's center-of-mass is shifted away from the center of the hub. Since 4-bladed rotor has two pairs of blades, hence, the sideward center-of-mass shift occurs twice per revolution. (ζ_{1c} is a lateral shift of rotor center-of-mass which results in 2/rev Y force. ζ_{1s} is a fore/aft shift of rotor center-of-mass which results in 2/rev H force. [2]) For a 6-bladed rotor, the side forces created will be 3rd harmonics.

Reduced Blade Flap Stiffness

Figure 4 presents the stability for a case when the flap stiffness (EI_Y) of one blade is reduced by 10%. Compared to the baseline results of Fig. 1, there is no discernable change in air resonance stability. Analysis shows that even the lag mode eigenvectors and modal frequencies are almost identical to the baseline case. Since flap modes damping are very high, so there is no need to worry that the flap modes can become unstable.

Figures 9 through 11 show negligible changes in any of the hub forces, except minute buildup of 2nd harmonic forces. However, Figs. 12 through 14 show large increase in first harmonic rolling, pitching and torque moments. The 1/rev moments are created because the single flapwise dissimilar blade tracks differently from the other blades. A single blade out of track always produce 1/rev vibrations. When the dissimilarity is in flapwise stiffness, the blades will flap differently, hence a rotor moment change is created. When the dissimliarity is in inplane stiffness, the rotor disk will not change its tilt, hence there is little change in rolling or pitching moment, and the 2nd harmonic side forces and torque change are solely inertia effects. Therefore, stability changes due to inplane stiffness dissimilarities can exist even in vacuum.

Unbalance Rotor Mass

The next dissimilar rotor case considered is when there is a mass unbalance. The total blades' mass is preserved at a constant, but one blade's mass is 10% less than the other three blades. The damping results for this case (Fig. 5) looks somewhat similar to the case when blade 1's lag stiffness is increased (Fig. 3). Both show similar improvement in regressing lag mode damping. This is due to reducing blade 2's mass is similar to increasing blade 2's inplane stiffness: both will increase blade 2's non-rotating lag frequency. If the time response for these two dissimilar rotors are plotted, they probably look very similar: both may show blade 2 has shorter period. On the other hand, increasing blade 2's mass will probably yield similar stability results as reducing blade 2's inplane stiffness.

Even though unbalanced mass rotor shows improved lag stability, but Figs. 9 through 14 show severe increase in all hub loads. This is expected because anytime a spinning rotor is unbalanced, severe 1/rev vibration is introduced from whirling of rotor center-

of-mass. As shown in Figs. 9 through 14, the inplane whirling of the unbalance mass rotor causes severe side forces; the 1/rev amplitude of H and Y forces are as high as 63% of the steady thrust force. Even the 1/rev rolling and pitching moments are 35 and 32% of the steady rotor torque.

Figures 16a through 16c show the time responses for the unbalanced mass rotor in hover. Figure 16a shows the initial lag displacement for all blades is 2°. Due to a reduction in blade mass, the oscillatory period for blade 2 is much shorter than other blades. The unbalanced mass configuration accentuates the coupling between blades and body motions. It only took two rotor revolutions for the unbalanced rotor to induce body pitch and roll oscillations. After 15 revolutions, the coupled blade/body responses become very chaotic. Even the flap and torsion responses in Figs. 16b and 16c show strong, unsteady, out of phase oscillations.

Reduced Blade Lift, $C_0 = C_0 - 0.1$

The last dissimilar rotor examined is what happens when aerodynamic lift of one blade is reduced. Blade 2's lift is reduced by subtracting 0.1 from its steady lift coefficient, $C_l = (C_0 - 0.1) + C_{l_\alpha}\alpha$. The consequence is as if the blade pitch link is adjusted inproperly which causes one blade out of track. As we already know from the reduced flap stiffness configuration, rotor tracking problem causes severe 1/rev rolling and pitching moments (Figs. 12 and 13). Noticeable 1/rev harmonic is seen in vertical force F_Z. This is simply because blade 2 produces less lift than other blades per revolution, hence a 1/rev lift variation. The strong 2/rev harmonics in H and Y side forces and moments are similar in nature to the 2/rev forces generated in inplane stiffness dissimilar rotor configurations. The inplane stiffness dissimilar rotors cause 2nd harmonic forces because the rotor center-of-mass shifts twice per revolution. In the lift dissimilar rotor configuration, the 2nd harmonics are due to two pairs of blades are flapping up and down in each revolution (β_{1c} causes M_y, and β_{1s} causes M_x). The moments are consequences of flapping, and side forces arise from lead-lag induced by flapping through coriolis.

Conservation of Total Energy Dissipation

It was mentioned earlier that when the stability of one mode is improved, the stability of other modes reduces. This conservation effect is best demonstrated in Table 3. Table 3 compares the sum of the decrement ratios for the baseline and dissimilar rotors at different advance ratios. Each number represents the sum of decrement ratio from all the lag modes. It can seen that at any advance ratio, the sum is almost the same among all rotors.

Conclusion

The aeromechanical stability and hub loads of five dissimilar rotors have been examined. It is observed that none of the dissimilar rotors worsen the regressing lag mode stability. On the contrary, some of the dissimilar rotor configurations improve lag mode stability. Specific conclusions that can be drawn from this investigation are:

1. Reducing or increasing the inplane stiffness of one blade improves regressing lag mode stability. But 2nd harmonic rotor drag and side forces are introduced due to rotor center-of-mass shifting twice per revolution. First harmonic torque load is also introduced.
2. Reducing the mass of one blade improves regressing lag stability, but increases all hub loads, especially 1/rev side forces and 1/rev pitching and rolling moments.
3. Reducing the flap stiffness does not affect aeromechanical stability and hub forces, it only increases 1/rev rolling and pitching moments.
4. Reducing the lift of one blade does not change aeromechanical stability, but increases all hub forces and moments.
5. For 4-bladed rotors, dissimilarities do not change 4/rev vibratory loads significantly, only 1st, 2nd, and 3rd harmonic hub loads are introduced.
6. The amount of "total" energy dissipation, or "total" damping in the system seems to be conserved. For all dissimilar rotor cases, when the stability of one mode is improved, the stability of another mode is decreased.
7. For dissimilar rotors, the time responses show all blades undergo different flap, lag, and torsional motions.
8. When the rotor is dissimilar, a substantial amount of coupling is introduced among all lag modes (progressing, regressing, collective, and differential modes).

Acknowledgements

The authors gratefully acknowledge the Army Research Office for supporting this research. The technical monitors are Dr. Robert Singleton, and Tom Doligalski.

Table 1: Rotor and Fuselage Data

Number of blades, N_b	4
Rotor radius, R	16.16 ft
Chord/Radius	.055
Lock number, γ	5.2
Solidity ratio, σ	.07
Nominal rotor speed, Ω_{ref}	424 rpm
Blade flap and lag inertia, I_b	161.9 slug-ft^2
Blade reference mass, m_0	0.1149 slug/ft
Airfoil,	NACA0012
Lift Coef., C_l	6.0α
Drag Coef., C_d	$.006 + .2\ \alpha^2$
Pitching moment, C_m	0.0
Blade linear twist, θ_{TW}	0°
Blade elastic axis	25 %
Blade CG location	25 %
Precone, β_p	0°
Rotor shaft height, h/R	0.2
Fuselage mass, $\frac{W}{gm_0R}$	77.24
Fuselage pitch inertia, $\frac{I_y}{m_0R^3}$	7.43
Fuselage roll inertia, $\frac{I_x}{m_0R^3}$	2.73

Table 2: Baseline Soft-Inplane Hingeless Blade Properties

Element	Flapwise $\frac{EI_y}{m_0\Omega^2R^4}$	Chordwise $\frac{EI_x}{m_0\Omega^2R^4}$	Torsion $\frac{GJ}{m_0\Omega^2R^4}$	Radius of Gyration $\frac{km}{R}$	Length $\frac{\ell}{R}$
1 – 4	.01080	.02680	.00615	.029	.20
5	.01080	.02680	.00615	.029	.18

Table 3: Sum of the Decrement Ratio

μ	Baseline rotor	Reduced blade 2 lag stiffness	Increased blade 2 lag stiffness	Reduced Blade 2 flap stiffness	Mass unbalance	Reduced blade 2 lift
0.0	.0274	.0271	.0277	.0279	.0268	.0289
0.1	.0170	.0169	.0173	.0174	.0166	.0179
0.2	.0168	.0166	.0171	.0172	.0165	.0177
0.3	.0292	.0288	.0291	.0291	.0279	.0293

References

[1] Wang, J. M., and Chopra, I., "Dynamics of Helicopters with Dissimilar Blades," presented at the 47th Annual National Forum of the American Helicopter Society, Phoenix, Arizona, May 1991.

[2] Wang, J. M., and Chopra, I., "Dynamics of Helicopters in Ground Resonance with and without Blade Dissimilarities," submitted for presention at the AIAA Dynamics Specialists Conference, April 16-17, 1992.

[3] Pierre, C., and Murphy, D. V., "Aeroelastic Modal Characteristics of Mistuned Blade Assemblies: Mode Localization and Loss of Eigenstructure," presented at the AIAA/ASME/ASCE/AHS/ASC 32nd Structural Dynamics and Materials Conference, Baltimore, Maryland, April 1991.

[4] Bendiksen, O. O., "Flutter of Mistuned Turbomachinery Rotors," *ASME Journal of Engineering for Gas Turbines and Power*, Vol. 106, 1984, pp. 25–33.

[5] Weller, W. H., and Peterson, R. L., "Measured and Calculated Inplane Stability Characteristics for an Advanced Bearingless Main Rotor," *Journal of the American Helicopter Society*, Vol. 29, (3), July, 1984.

[6] Hammond, C. E., "An Application of Floquet Theory to Prediction of Mechanical Instability," *Journal of the American Helicopter Society*, Vol. 19, (4), Oct. 1974, pp. 14–23.

[7] McNulty, M. J., "Effects of Blade-to-Blade Dissimilarities on Rotor-body Lead-lag Dynamics," *Journal of the American Helicopter Society*, Vol. 33, (1), Jan. 1988, pp. 17–28.

[8] Wang, J. M., Jang, J., and Chopra, I., "Air Resonance Stability of Hingeless Rotors in Forward Flight'" *Vertica*, Vol. 14, (2), 1990, pp. 123–136.

[9] Bir, G. S., Chopra, I. and Khanh, N., "Development of UMARC (University of Maryland Advanced Rotorcraft Code)," presented at the 46th Annual National Forum of the American Helicopter Society, Washington, D. C., May 1990.

[10] Ormiston, R. A., "Rotor-Fuselage Dynamic Coupling Characteristics of Helicopter Air and Ground Resonance," *Journal of the American Helicopter Society*, Vol. 36, (2), April 1991, pp. 3–20.

[11] Johnson, W., *"Helicopter Theory,"* Princeton University Press, Princeton, New Jersey, 1980, pp. 361–364.

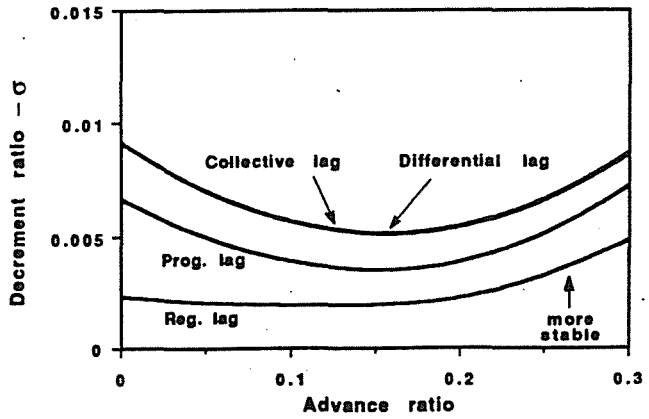

Figure 1 Baseline soft-inplane hingeless rotor.

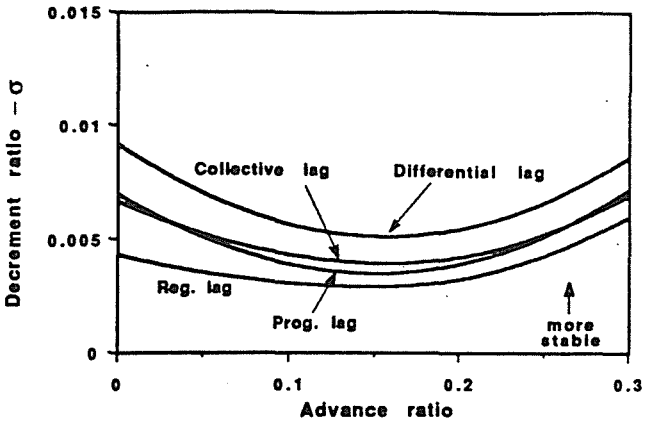

Figure 2 Reduced one blade's lag stiffness by 10%.

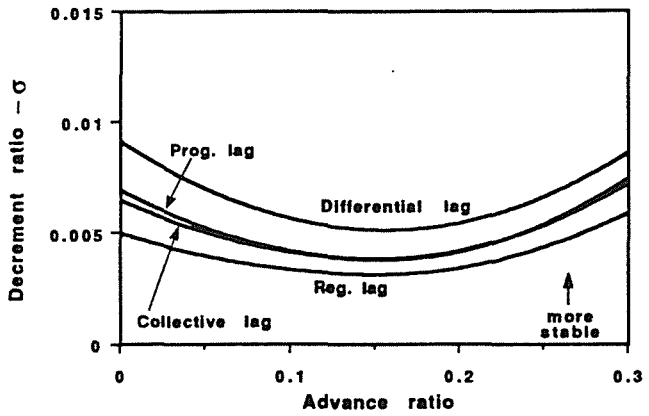

Figure 3 Increased one blade's lag stiffness by 10%.

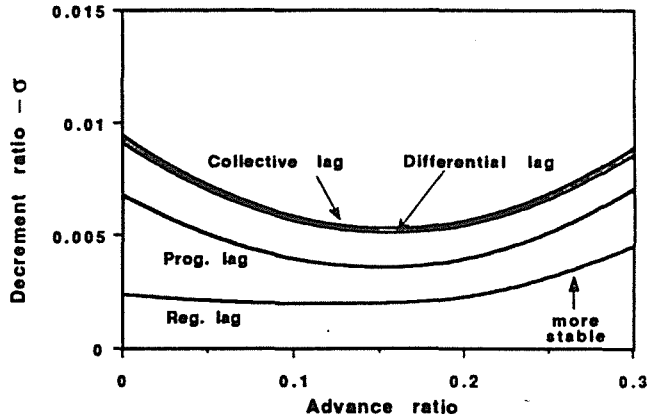

Figure 4 Reduced one blade's flap stiffness by 10%.

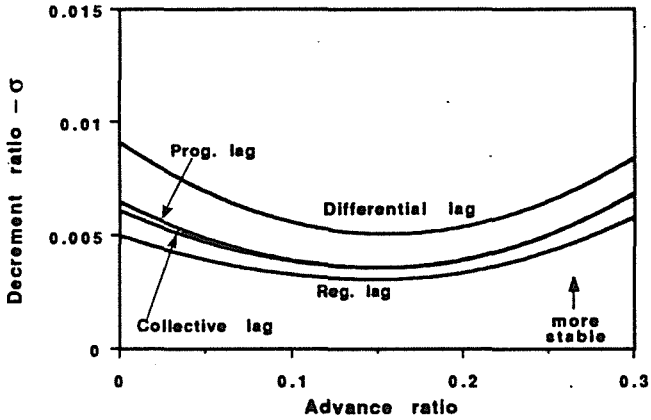

Figure 5 Reduced one blade's mass by 10%.

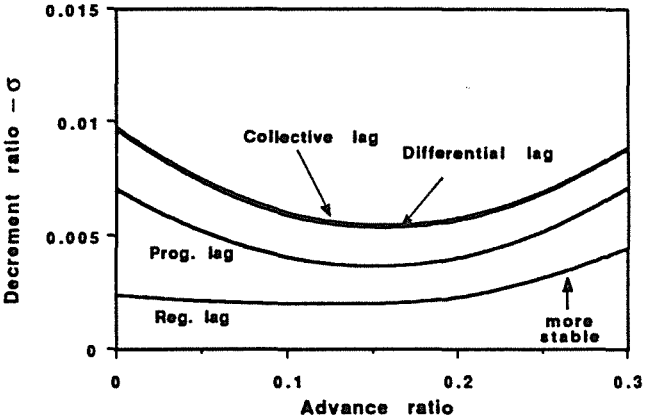

Figure 6 Reduced one blade's lift Co = Co - 0.1

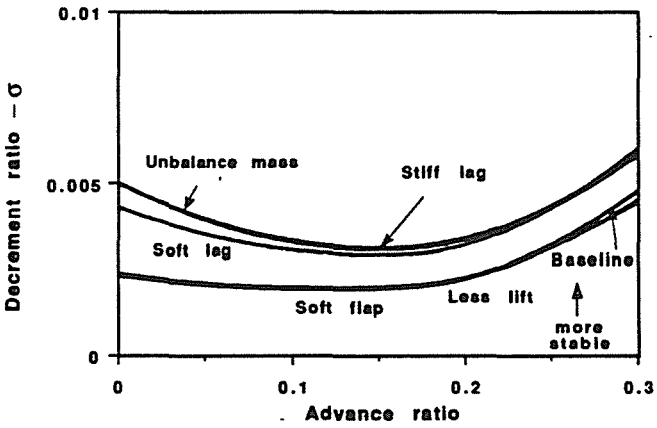

Figure 7 Comparing regressing lag modes' stability.

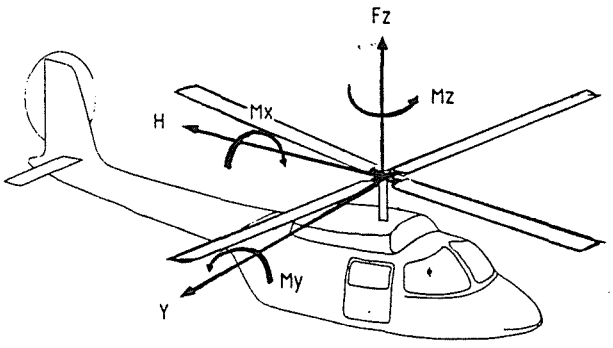

Figure 8 Rotor hub loads in nonrotating frame: H = drag force, Y = side force, Fz = vertical force, Mx = rolling moment, My = pitching moment, Mz = torque.

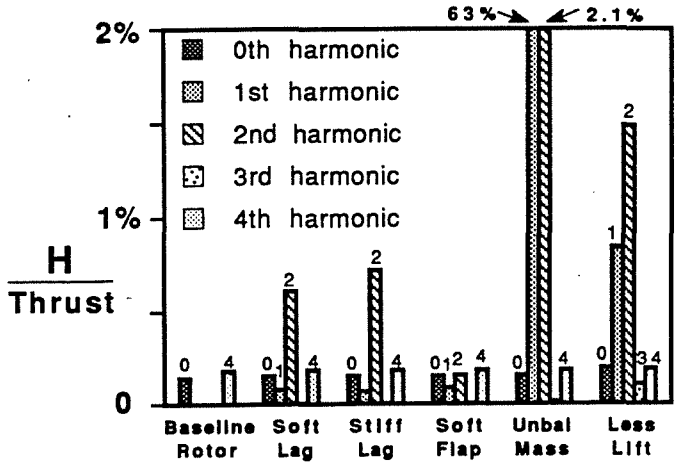

Figure 9 Harmonics of rotor drag force at $\mu = 0.2$

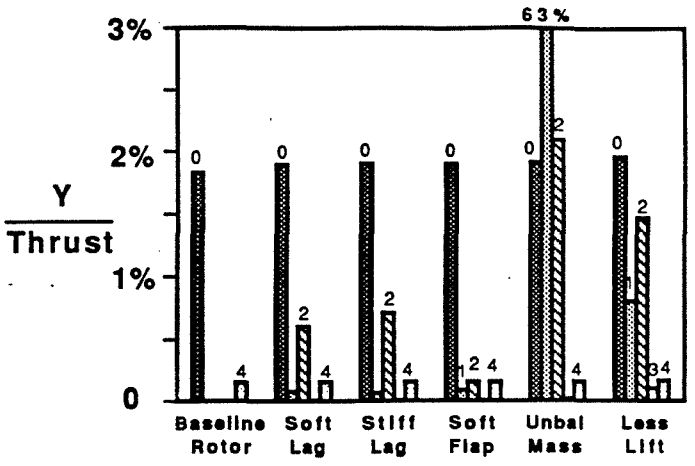

Figure10 Harmonics of rotor side force at $\mu = 0.2$

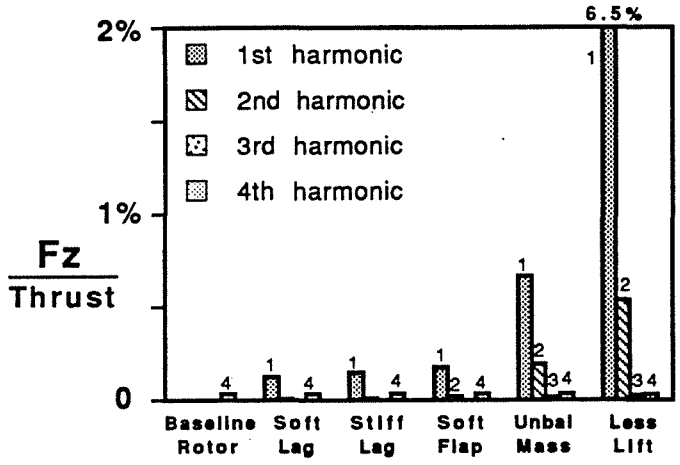

Figure 11 Harmonics of vertical force at $\mu = 0.2$

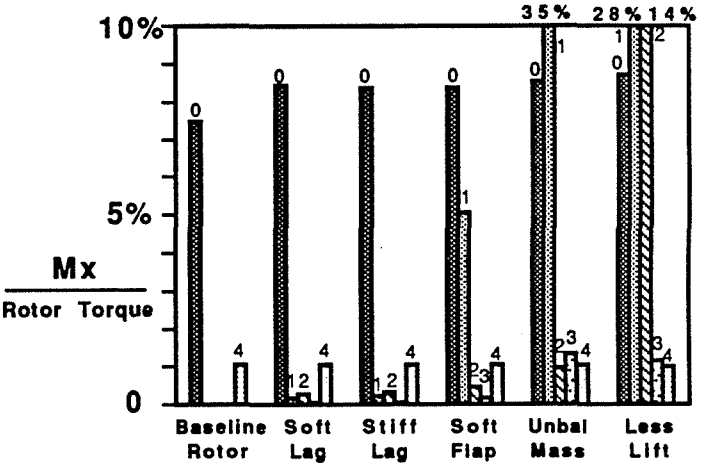

Figure 12 Harmonics of rotor rolling moment at $\mu = 0.2$

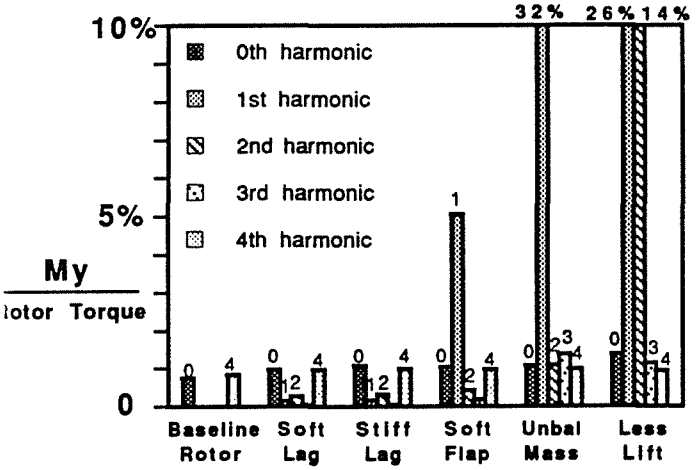

Figure 13 Harmonics of rotor pitching moment at $\mu = 0.2$

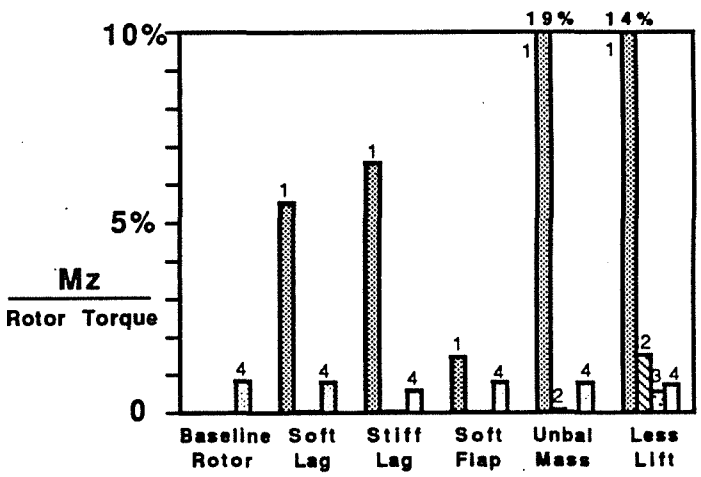

Figure 14 Harmonics of rotor torque at $\mu = 0.2$

Responses from time integration of the coupled blades/body linearized perturbation equations. An initial lag displacement of 2 degrees is given to all four blades. Hover, rpm = 420, Ct/sigma = 0.07

For a dissimilar rotor with 10% less inplane stiffness for one blade.

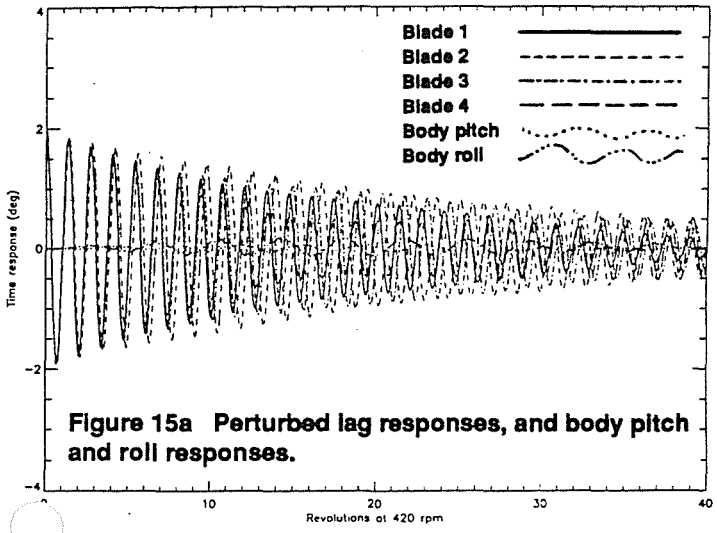

Figure 15a Perturbed lag responses, and body pitch and roll responses.

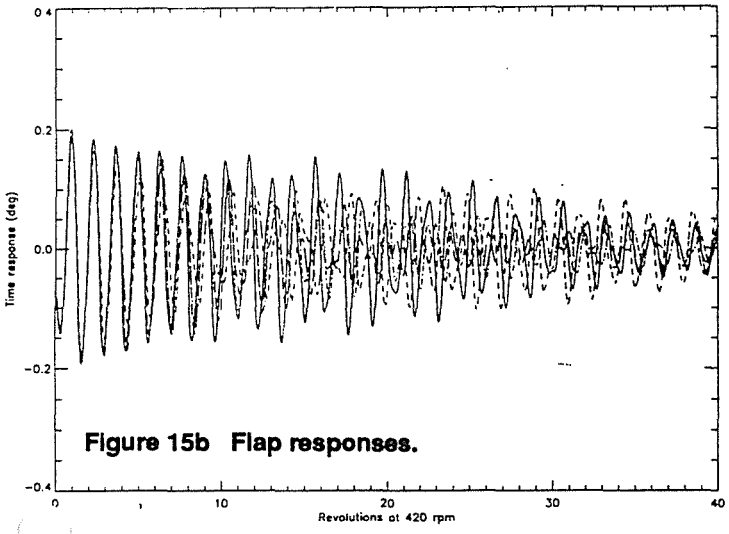

Figure 15b Flap responses.

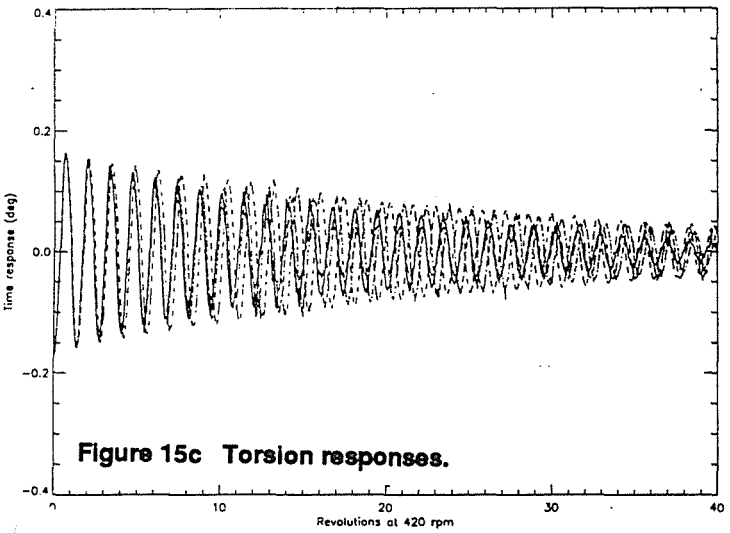

Figure 15c Torsion responses.

For a dissimilar rotor with 10% less mass for one blade.

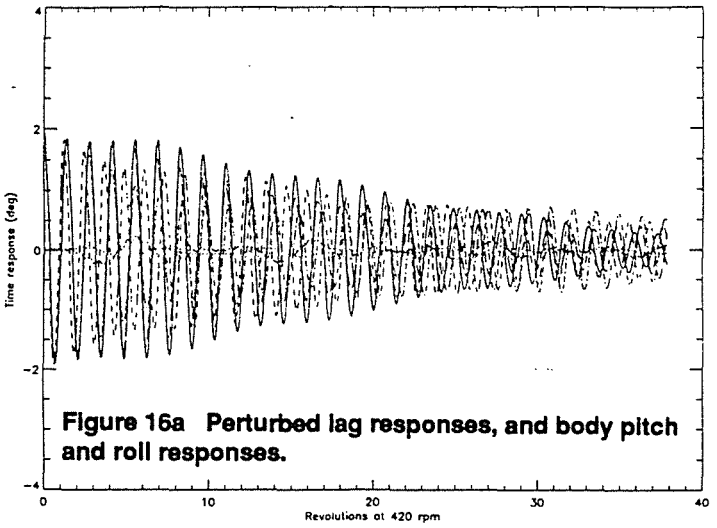

Figure 16a Perturbed lag responses, and body pitch and roll responses.

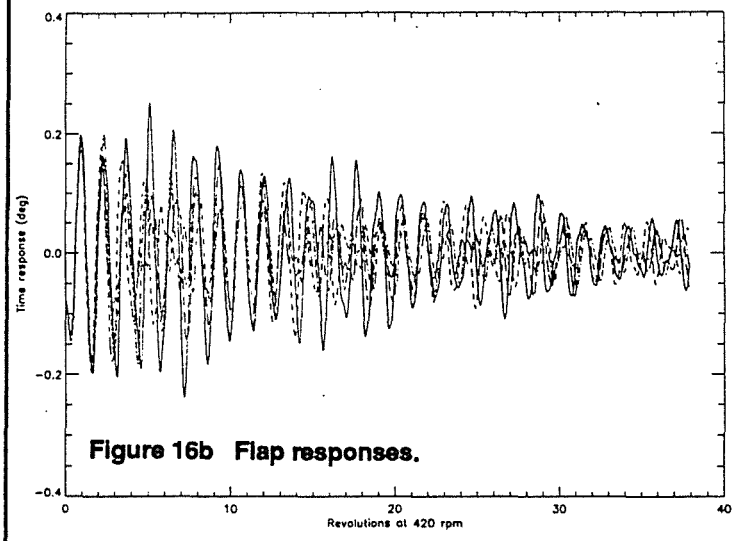

Figure 16b Flap responses.

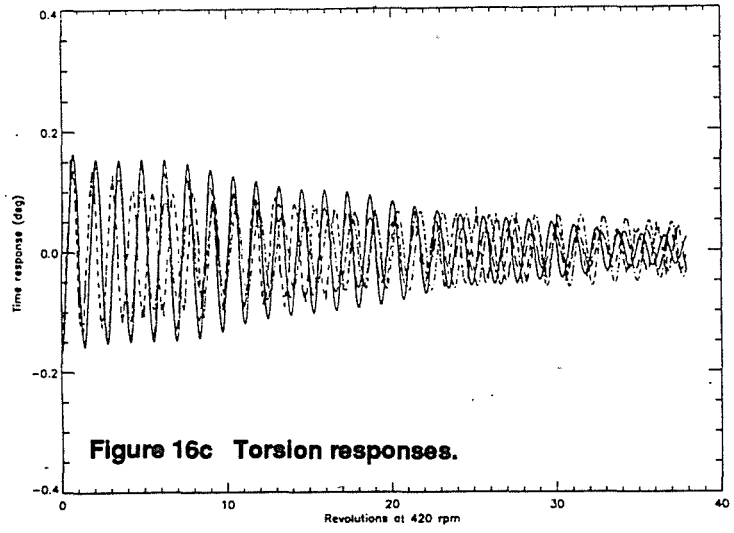

Figure 16c Torsion responses.